# Circular dichroism from unpolarized atoms in multiphoton multicolor ionization

Richard Taïeb, Valérie Véniard, and Alfred Maquet
*Laboratoire de Chimie Physique-Matière et Rayonnement, Université Pierre et Marie Curie, 11, Rue Pierre et Marie Curie, 75231 Paris Cedex 05, France*

N. L. Manakov and S. I. Marmo
*Department of Physics, Voronezh State University, 394693 Voronezh, Russia*
(Received 7 January 2000; published 7 June 2000)

The angular distribution of the photoelectrons produced from a ground-state atom ionized under the combined action of two (or several) radiation fields can exhibit circular dichroism effects, when reversing the polarization state (right versus left, for instance) of one of the fields. We address the question of such dichroic effects in a currently explored scenario in which the atom is ionized in the presence of a strong laser field and of one (or several) of its higher harmonics.

PACS number(s): 32.80.Rm, 32.80.Fb, 03.65.Pm

## I. INTRODUCTION

Circular dichroism–based spectroscopic studies are recognized as a valuable tool to investigate structural effects in the response of chiral systems to an electromagnetic field. For such systems, the dependence of the (one-photon) photoionization differential cross sections on the helicity of the field is well documented [1]. It is also known that dichroic effects can be observed in the (one-photon) double photoionization of nonchiral systems, the simpler being a ground-state helium atom [2]. This process has attracted a lot of attention, since recent experimental measurements [3] provide a very sensitive test of the importance of electron correlations in multielectron systems [4]. Spectacular developments, relying on the advent of third generation synchrotron sources, have also been recently registered in the analysis of resonant x-ray scattering spectra from magnetic solids [5].

It is not so widely known that the relative magnitudes and phases of the transition amplitudes governing the nonlinear response of nonchiral systems, typically a ground-state atom, can be also derived from the analysis of dichroic signals obtained from multiphoton processes. In single-color processes no dichroism is observed if one limits oneself to (left- or right-) circular polarization states. By contrast, elliptical dichroism in multiphoton ionization has been observed in the angular distributions of photoelectrons originating from rare gas samples [6]; see also the discussions in Ref. [7]. The question has been addressed also in other instances, see, for example, Refs. [8], and [9], the latter being dedicated to the discussion of a special geometry in relation to experiments. A recent theoretical study, including the general treatment of elliptical dichroism in two-photon ionization of atoms, with no restriction either on the detection geometry or on the propagation directions of the fields, can be found in Ref. [10].

The potential interest in multiphoton dichroic measurements on atoms results from a general property of the associated dipole ionization amplitudes, namely on the fact that they contain several components associated to different (in general interfering) quantum paths leading to the final state. In multiphoton ionization experiments, the contributions of different final angular momentum states of the photoelectrons are not resolved and it is only possible (for instance, through a fit in terms of Legendre polynomials), to get a qualitative picture of the relative magnitudes of the various transition amplitudes [11,12]. Within this context, the main advantage of dichroic measurements with elliptically polarized light is that one can, in principle, determine the relative magnitudes and phases of the various interfering transition amplitudes, via the analysis of the photoelectron angular distributions obtained for different polarization states of the fields [9]. Such data are of major interest for addressing interesting issues, such as of the role of multiphoton propensity rules [13] related to the highly nonlinear response of atomic systems in strong laser fields.

The motivation of this paper is to draw attention to the possibility of obtaining similar information with the help of two-color (or, more generally, multicolor) schemes, the fields having different polarization states. As already mentioned, a very general theoretical analysis of elliptical dichroism in two-photon ionization processes, has been presented recently [10]. Here, we wish to present an extension of this analysis to the case of the circular dichroism effects in *two- and three-color* absorption processes leading to *two- and/or three-photon* ionization. Although elliptical dichroism is potentially richer in information, we shall restrict the discussion here to the simpler case of circular dichroism which allows us to illustrate the main features of the effect. Moreover, we shall consider a specialized geometry which has been chosen, for the sake of comparison, with currently planned experiments with higher harmonics [14]. We note that a complete analytical treatment of multiphoton transitions involving two or more fields with distinct polarization states would entail prohibitively cumbersome computations. In any case, it would result in general formulas from which it would be difficult to extract physical insights on the mechanisms governing the atomic response. Instead, we have considered the special case of ionization of a ground *s*-state atom under the combined effects of a circularly polarized laser field and of the linearly polarized field of a higher harmonic of the fundamental. Then, the symmetry properties and the overall angular distribution of the photoelectrons can be derived in

 

closed form. We should mention also that the scenario we have chosen takes advantage of the properties of the harmonic radiations generated in rare gas irradiated by a strong IR laser. In the present context, the main advantage of these recently developed sources of XUV radiation is, in addition to their coherence and high brightness, the brevity of the pulse which is synchronized with the laser pump pulse [15].

When an atomic system is submitted simultaneously to a radiation pulse containing several frequencies, it can exchange (absorb or emit, via stimulated emission) photons with each of the fields. Here, we shall consider the case of a strong IR laser and of one or two of its higher harmonics. Then, as a consequence of the intrinsically much lower intensity of the harmonic field, the atom-harmonic interaction is dominated by single-photon absorption. In contrast, the exchange of several IR photons can take place, even at moderate laser intensities around $10^{12}$ W/cm$^2$ [16–18]. The practical realization of such a scenario must take into account the fact that, in actual harmonic generation devices, the harmonic radiation is emitted in the forward direction and is linearly polarized parallel to the polarization direction of the laser pump field [15]. With suitable optical devices, it is then feasible to split the two beams and to change the polarization state of the laser (a much easier task than for the harmonic light) before to make them to merge again on the atomic sample. Here we shall consider two- and three-color photoionization processes induced by the simultaneous absorption of one photon from the (linearly polarized) harmonic field and from at least one photon from the (circularly polarized) laser field. As we shall show below, depending on the (right- or left-) circular polarization state of the laser, the angular distribution of the photoelectrons are modified. If the harmonic frequency is high enough, so that above-threshold ionization (ATI) can take place [16–18], additional modifications can be evidenced in the dichroic signal.

We shall show also that one can take advantage of another feature of harmonic spectra, namely that they contain lines regularly spaced in frequency, separated by $2\omega_L$, where $\omega_L$ is the frequency of the pump laser. If the atom is irradiated by such a ''Dirac comb'' of frequencies, new interfering paths are open and additional dichroic features are expected to appear.

The paper is organized as follows. In Secs. II and III we present the theoretical background needed to discuss the dichroic effects which are expected to take place when performing experiments along the lines of the above described scenario involving either two (Sec. II) or three (Sec. III) photons. We shall present also some numerical data deduced from a perturbative treatment of the problem for a hydrogen atom initially in its ground state. Although much simplified, the model contains all the ingredients needed for discussing the main features of this class of dichroic phenomena. The conclusions will be presented in Sec. IV.

## II. TWO-PHOTON, TWO- AND THREE-COLOR IONIZATION

### A. Theoretical background

In order to present the formalism, we shall first address the simpler case of two-photon ionization involving the simultaneous absorption of one high frequency photon (the harmonic) and of one low frequency photon from the laser. The frequencies of the laser $\omega_L$ and of the harmonic $\omega_H$ are such that $\omega_L+\omega_H>|E_0|$, where $E_0$ is the ground-state energy of the atom. We note that if $\omega_H>|E_0|$, ATI can take place. As we shall show below, the angular dependence of the dichroic effect can be substantially modified as compared to the case when $\omega_H<|E_0|$.

In the presence of the two fields, either the laser photon or the harmonic can be absorbed first. As a consequence, one has to add coherently the two interfering amplitudes associated to each path leading to the same final quantum state. Here, the final state belongs to the continuous spectrum of the atom and, when recording the angular dependence of the photoionization process, one detects photoelectrons propagating with a definite wave vector $\mathbf{k}$. Such states will be labeled by their wave number $k$, such as $k=\sqrt{2E_k}$ where $E_k$ is the kinetic energy of the photoelectron and, neglecting very small spin effects, by their angular momentum quantum numbers $(L,M)$. It is then convenient to express the wave function in terms of a partial wave expansion which reads, in the special case of hydrogen

$$\langle \mathbf{r}|\phi_{\mathbf{k}}\rangle = C_k \sum_{L=0}^{+\infty} i^L e^{-i\eta_L} R_{k,L}(r) \sum_{M=-L}^{+L} Y_{L,M}(\hat{\mathbf{r}}) Y^*_{L,M}(\hat{\mathbf{k}}), \tag{1}$$

where $C_k$ is a normalization constant, $\eta_L$ is the Coulomb phase shift, $\eta_L=\arg\Gamma(L+1-i/k)$, $R_{k,L}(r)$ is the (real) radial wave function for angular momentum $L$, and the angular functions $Y_{L,M}$ are spherical harmonics. When starting from the hydrogen ground state, the two-color, two-photon transition amplitudes are expressed in terms of the two following second-order atomic matrix elements:

$$M_A = \langle \phi_{\mathbf{k}}|\hat{\boldsymbol{\epsilon}}_L\cdot\mathbf{r} G(\Omega_A)\hat{\boldsymbol{\epsilon}}_H\cdot\mathbf{r}|\phi_{1s}\rangle, \tag{2}$$

which corresponds to processes in the course of which the harmonic photon is absorbed first and

$$M_B = \langle \phi_{\mathbf{k}}|\hat{\boldsymbol{\epsilon}}_H\cdot\mathbf{r} G(\Omega_B)\hat{\boldsymbol{\epsilon}}_L\cdot\mathbf{r}|\phi_{1s}\rangle, \tag{3}$$

which corresponds to the case where it is the laser photon which is absorbed first. In these expressions, $G(\Omega)$ stands for the Coulomb Green's function [19], with the arguments $\Omega_A=E_0+\omega_H$ and $\Omega_B=E_0+\omega_L$. Here, the (in general complex) vectors $\hat{\boldsymbol{\epsilon}}_L$ and $\hat{\boldsymbol{\epsilon}}_H$ are unit polarization vectors of the IR and UV photons, respectively.

The partial wave expansions for these amplitude are straightforwardly derived as

$$M_A = C_k^* \sum_{L=0,2} (-i)^L e^{+i\eta_L} T_L(\Omega_A) \times \sum_{M=-L}^{+L} Y_{L,M}(\hat{\mathbf{k}}) \sum_{\mu=-1}^{+1} C_{L,M,\mu}, \tag{4}$$

and a similar expression for $M_B$. Here the coefficients $C_{L,M,\mu}$ contain standard products of Wigner 3-$j$ symbols,

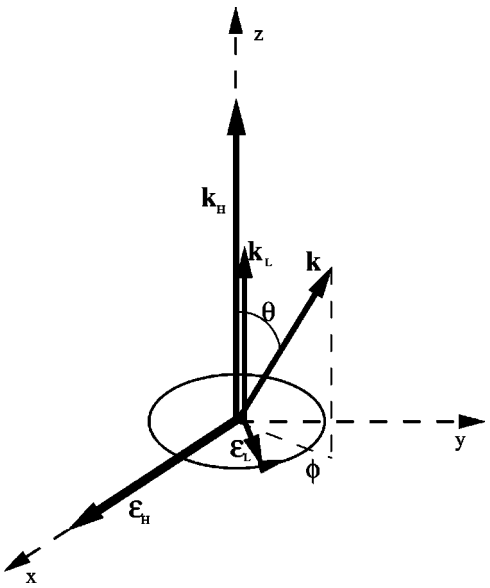


FIG. 1. Geometry used in the computations. The fields' wavevectors ($\mathbf{k}_L$,$\mathbf{k}_H$) are along the quantization axis ($Oz$), while the harmonic polarization $\boldsymbol{\epsilon}_H$ is along the $Ox$ axis and the laser polarization $\boldsymbol{\epsilon}_L$ ''turns'' in the $xOy$ plane. The photoelectron wave vector $\mathbf{k}$ as well as the angles $\theta=(\widehat{Oz,\mathbf{k}})$ and $\phi$ are also shown.

and the quantities $T_L(\Omega)$ are second-order reduced radial amplitudes of the general form:

$$T_L(\Omega)=\langle R_{k,L}|rG_1(\Omega)r|R_{1s}\rangle, \tag{5}$$

where $G_1(\Omega)$ is the radial component of the Coulomb Green's function for angular momentum $\lambda=1$.

Another useful representation of the second-order amplitudes, very convenient for discussing the general properties of the angular dependence of the amplitudes is (see, e.g., [10] for more details),

$$M_A=\frac{C_k^*}{3\sqrt{4\pi}}\{e^{i\eta_0}T_0(\Omega_A)\hat{\boldsymbol{\epsilon}}_L\cdot\hat{\boldsymbol{\epsilon}}_H+e^{i\eta_2}T_2(\Omega_A)\times[\hat{\boldsymbol{\epsilon}}_L\cdot\hat{\boldsymbol{\epsilon}}_H-3(\hat{\boldsymbol{\epsilon}}_L\cdot\hat{\mathbf{k}})(\hat{\boldsymbol{\epsilon}}_H\cdot\hat{\mathbf{k}})]\}, \tag{6}$$

and a similar expression for $M_B$.

For the sake of further reference, we note that when the argument $\Omega<0$, the radial matrix elements $T_L(\Omega)$ are real valued, while if $\Omega>0$, they become complex [19]. Here, the latter situation can occur specially in the matrix element labeled $A$ when $\omega_H>|E_0|$. Then, one-photon ionization can take place, through the absorption of one harmonic photon, and ATI can be observed. This shows that, in the presence of ATI, an additional complex phase factor is included in the matrix element $M_A$, as compared to the case when $\omega_H<|E_0|$. Before to come back to this point in the discussion below, we turn now to derivation of the explicit form of the angular distribution of the photoelectrons in the above-mentioned specialized geometry.

In the following, we shall assume that the two beams are parallel, propagating along the $Oz$ axis, see Fig. 1. The linear polarization vector of the harmonic is oriented along the $Ox$ axis, $\boldsymbol{\epsilon}_H=\hat{\mathbf{x}}$, while the circular polarization vector of the laser is in the $xOy$ plane,

$$\boldsymbol{\epsilon}_L^{\pm}=\frac{1}{\sqrt{2}}(\hat{\mathbf{x}}\pm i\hat{\mathbf{y}}).$$

Using standard techniques of angular momentum algebra, it is an easy matter to determine the accessible final quantum states, depending on the polarization state of the laser. For the chosen geometry, and starting from an $s$ state $(l,m)=(0,0)$, the photoelectron can occupy the following angular momentum states: $(L,M)=(0,0)$, $(2,0)$, and $(2,\pm 2)$. Here, the sign $\pm$ in the last entry depends on the (left or right) circular polarization of the field. Obviously, circular dichroism effects originate from this difference of sign. It is an easy matter to obtain the differential cross sections:

$$\frac{d\sigma^{\pm}}{d\Omega(\theta,\phi)}=\frac{\pi k}{8}I_L I_H|M_A^{\pm}+M_B^{\pm}|^2, \tag{7}$$

where $I_L$ and $I_H$ represent the intensities of the laser and of the harmonic, expressed in atomic units, i.e., in terms of $I_0=3.5\times 10^{16}$ W/cm$^2$. Then, from either expression, Eqs. (4) or (6), one can derive its variations in terms of the azimutal ($\phi$) and polar ($\theta$) angles of the ejected photoelectrons, for each polarization state of the laser field,

$$\frac{d\sigma^{\pm}}{d\Omega(\theta,\phi)}\propto A_1+A_2\sin^4\theta\cos^2\phi+A_3\sin^2\theta\cos^2\phi \pm A_4\sin^2\theta\sin(2\phi), \tag{8}$$

where the invariant atomic parameters $A_J$ are

$$A_1=|T_0|^2+|T_2|^2+2\,\mathrm{Re}\{e^{i(\eta_2-\eta_0)}T_0^*T_2\},$$
$$A_2=9|T_2|^2,$$
$$A_3=-6[\mathrm{Re}\{e^{i(\eta_2-\eta_0)}T_0^*T_2\}+|T_2|^2],$$
$$A_4=3\,\mathrm{Im}\{e^{i(\eta_2-\eta_0)}T_0^*T_2\}. \tag{9}$$

Here, $T_L$, $(L=0,2)$, denotes the combined radial amplitudes:

$$T_L=T_L(\Omega_A)+T_L(\Omega_B). \tag{10}$$

It appears that, in the chosen geometry, dichroism effects can be observed only in the $\phi$ dependence of the last term in this expression of the cross section. More precisely, the difference between the cross sections for the right and left circular polarization states reduces to

$$\frac{d\sigma^{+}}{d\Omega(\theta,\phi)}-\frac{d\sigma^{-}}{d\Omega(\theta,\phi)}\propto T_0T_2\sin^2\theta\sin(\eta_2-\eta_0)\sin(2\phi). \tag{11}$$

This result shows that, for $s$ states and for the chosen geometry, dichroic effects are maximized when detecting the photoelectrons in the plane $xOy$, $(\theta=\pi/2)$, i.e., in the plane

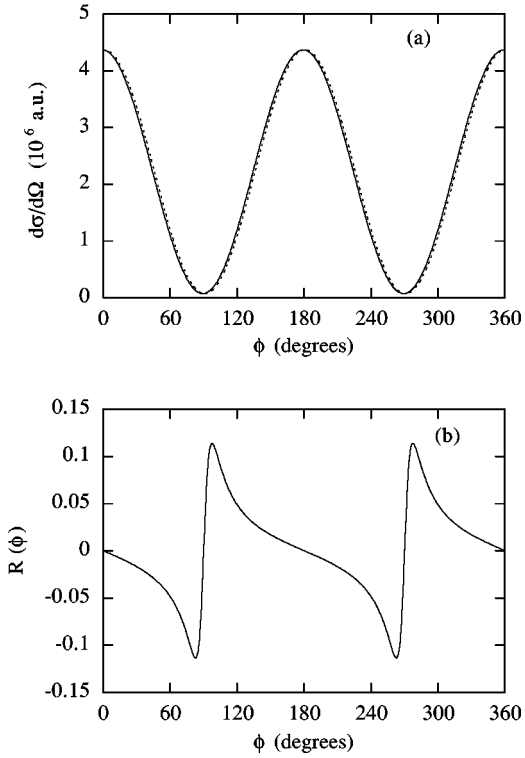


FIG. 2. Differential cross section $d\sigma/d\Omega$ in a.u. and the corresponding dichroic signal $R(\phi)$ as a function of the azimuthal angle $\phi$ for the absorption from the hydrogen atom ground state $(1s)$ of a circularly polarized laser photon with energy $\omega_L=1.4$ eV and a linearly polarized harmonic photon with energy $\omega_H=9\omega_L$. The corresponding intensities were taken, for simplicity, to be equal to 1 a.u. The geometry is shown in Fig. 1, with $\theta=90°$. (a) The full line corresponds to the differential cross section for right-polarization, while the left-polarization case is shown in dotted line. (b) dichroic signal as defined in Eq. (12).

containing the polarization vectors of the two fields. On the contrary, there is no dichroism when the photoelectrons are ejected either parallel or perpendicular to the linear polarization vector of the harmonic field, i.e., for $\phi=0$ or $\phi=\pi/2$. Moreover, one observes that the dichroic signal, usually defined as

$$R(\phi)=\frac{\dfrac{d\sigma^+}{d\Omega}-\dfrac{d\sigma^-}{d\Omega}}{\dfrac{d\sigma^+}{d\Omega}+\dfrac{d\sigma^-}{d\Omega}}, \tag{12}$$

exhibits the following $\phi$ dependence for $\theta=\pi/2$:

$$R(\phi)\propto\frac{\sin(2\phi)}{\alpha_1+\alpha_2\cos(2\phi)}, \tag{13}$$

and changes sign when $\phi$ varies around $\pi/2$ (see the discussion below). Here, the quantities $\alpha_1$ and $\alpha_2$ are expressed in terms of the atomic parameters $A_J$ $(J=1,4)$ [see Eqs. (8) and (9)].

Another interesting point is that the magnitude of the dichroic effects are $k$ dependent through the Coulomb phase shifts difference:

$$\eta_2-\eta_0=\arctan(3k/2k^2-1),$$

in Eq. (11). In particular, they are suppressed in the limit when the latter becomes small. This happens in two distinct physical situations: (i) for $k\to\infty$, i.e., for high energy photoelectrons. In other words, as already noted in similar contexts, dichroic effects become vanishingly small if the conditions of applicability of the first Born approximation are met [7–9]. (ii) When $k\to0$, i.e., for threshold photoelectrons the dichroism vanishes also. Between these two limits, it then appears that the dichroic difference, Eq. (11), becomes maximum around $k=1/\sqrt{2}$. We stress that although this result has been established for hydrogen, it is general and should apply, with suitably modified phase shifts, to the case of complex atoms. This implies also that dichroism might be a useful spectroscopic tool for determining such phase shifts.

In the preceding analysis it has been implicitly assumed that the second-order radial matrix elements, Eq. (5), were real. This corresponds to the case $\omega_H<|E_0|$. However, as already mentioned, if $\omega_H>|E_0|$, some of the amplitudes $T_L$ becomes complex and acquires a phase: $T_L\to|T_L|\exp(i\theta_L)$. The consequence is that the general form of the dichroic difference becomes:

$$\frac{d\sigma^+}{d\Omega(\theta,\phi)}-\frac{d\sigma^-}{d\Omega(\theta,\phi)}\propto|T_0T_2|\sin^2\theta\sin(\eta_2+\theta_2-\eta_0-\theta_0)\sin(2\phi). \tag{14}$$

This clearly shows that the magnitude of the dichroic signal can be significantly modified, depending if whether ATI can take place or not. This point will be illustrated below.

For two-photon ionization processes originating from other, non-$s$ states, the angular analysis is more involved and simple formulas as, in Eqs. (11) or (14), are not easy to establish; see [10]. For instance, for non-$s$ states the general form of the angular distribution, generalizing Eq. (8), involves nine independent, invariant, atomic parameters $A_J$ (instead of six for one-color ionization [10]). The difficulty is even more considerable for higher-order *two-color* multiphoton ionization processes. Already for three-photon transitions, the formalism becomes extremely intricate [20], and it is much more convenient to directly perform a numerical computation of the matrix elements. We turn now to the presentation of such numerical data for two- and three-photon ionization processes, in the presence of several radiation fields. We mention that the corresponding transition amplitudes have been computed with the help of a sturmian approach already used in other instances [21]. In the discussion, we shall address the question of the choice of the detection geometry and more generally of the conditions required in order to optimize the observation of this class of dichroic effects.

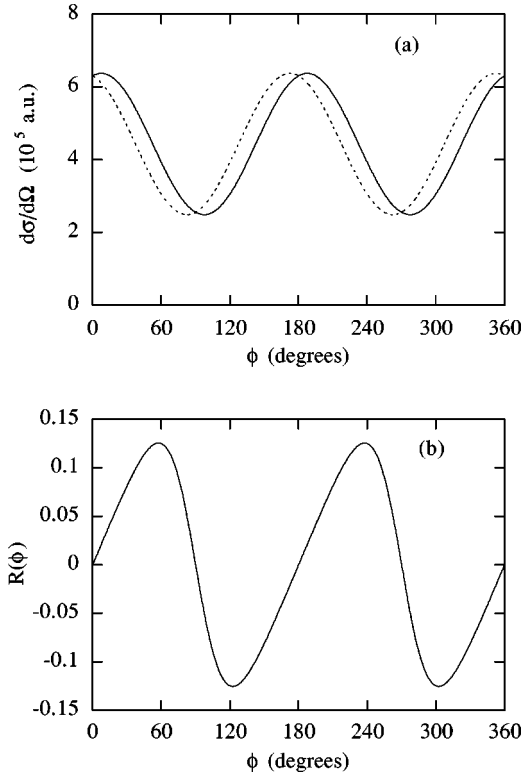


FIG. 3. Same as Fig. 2 with $\omega_L = 1.361$ eV.

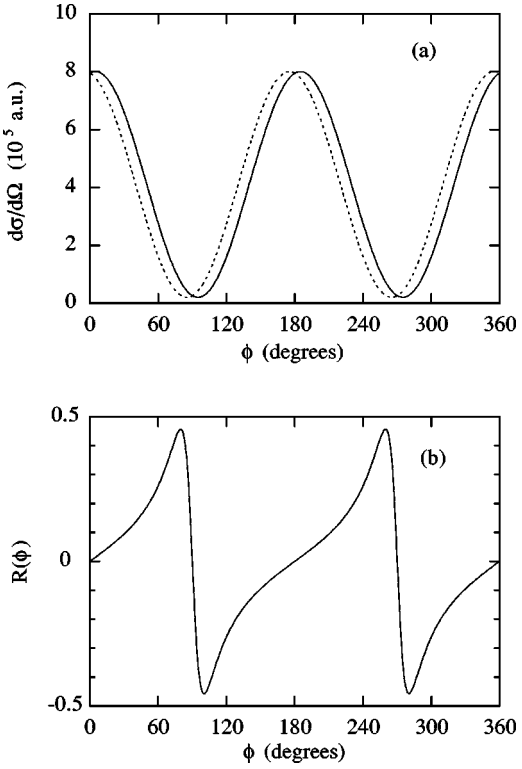


FIG. 4. Same as Fig. 2 with $\omega_L = 1.55$ eV (Ti:sapphire laser).

### B. Numerical results and discussion: Two-color, two-photon ionization

In order to illustrate the above concepts, we have considered first the simpler case of two-photon ionization of H($1s$), resulting in the simultaneous absorption of one (circularly polarized) low-frequency photon $\omega_L$ and of one (linearly polarized) high-frequency photon, $\omega_H$. The geometry is displayed in the Fig. 1. Hereafter, the angle $\theta$ is being chosen as $\theta = 90°$. Even for this simple process, we have to consider two distinct cases according to the following.

(i) $\omega_H < |E_0|$, i.e., single-photon ionization is forbidden. This scenario can be difficult to realize in experiments with IR lasers, since the photoelectrons are intrinsically slow, with energies below $\omega_L$, which can make analysis difficult. We have nevertheless addressed the question as it displays interesting characteristics. This is illustrated in Figs. 2(a) and 2(b), where the differential cross sections and the dichroic signals are reported in terms of $\phi$ for $\omega_L = 1.4$ eV and $\omega_H = 9\omega_L$, i.e. $\omega_L + \omega_H = 14$ eV. We note, see Fig. 2(b), that although the dichroic difference, Eq. (9), has a trivial $\sin(2\phi)$ dependence, the scaled dichroic signal $R(\phi)$, Eq. (11), exhibits a typical dispersionlike shape, the maximum contrast being slightly larger than 10%.

For threshold photoelectrons, as they would be obtained with $\omega_H + \omega_L \approx |E_0|$, the cross sections not only remain finite but, in fact, take their maximum value [22]. One could think of taking advantage of this fact for performing dichroic measurements on slow photoelectrons in order to increase the counting rates. Unfortunately, because of the dependence of the dichroic difference, Eq. (9), on the Coulomb phase shifts, the difference goes to zero with the electron wave number $k$, as arctan($3k$). The result is that the dichroic signal is practically not enhanced when performing experiments with slow electrons. This point is illustrated in Fig. 3, for $\omega_L = 1.361$ eV and $\omega_H = 9\omega_L$, i.e., for very slow photoelectrons with kinetic energy $k^2/2 \approx 0.5$ meV. In comparison with the Fig. 2, one observes that, although the cross section is significantly larger, the dichroic contrast does not increase.

Another feature of this class of two-photon ionization processes is that the *maxima* of the dichoic signals are located very close to the *minima* of the cross sections. This feature might preclude an easy experimental determination of the dichroic ratio. As we shall show next, the situation can be slightly improved when ATI can take place.

(ii) $\omega_H > |E_0|$, i.e., single-photon ionization is permitted and ATI can be observed. In this case, the radial matrix elements become complex and the maxima of the dichroic ratios are shifted, as compared to the preceding situation. This results from the convolution of the $\phi$ dependence of the cross section with dichroic differences whose magnitudes are changed with respect to the preceding case, see Eq. (11).

To illustrate this scenario we have considered a laser frequency $\omega_L = 1.55$ eV (Ti:sapphire laser), and two of its harmonics: $\omega_H = 9\omega_L$, (H9), see Figs. 4(a) and 4(b), and $\omega_H = 11\omega_L$, (H11), see Figs. 5(a) and 5(b). Here also the dichroic signals exhibit the familiar dispersionlike shape, the maxima being significantly higher than in the preceding cases: it is close to 0.5 for H9, see Fig. 4(b), and just above 0.3 for H11, see Fig. 5(b). For higher harmonics, the contrast in the dichroic signal continues to decrease. Unfortunately, the dichroic maxima are still located close to the minima of the cross sections, as shown in the figures. The situation is

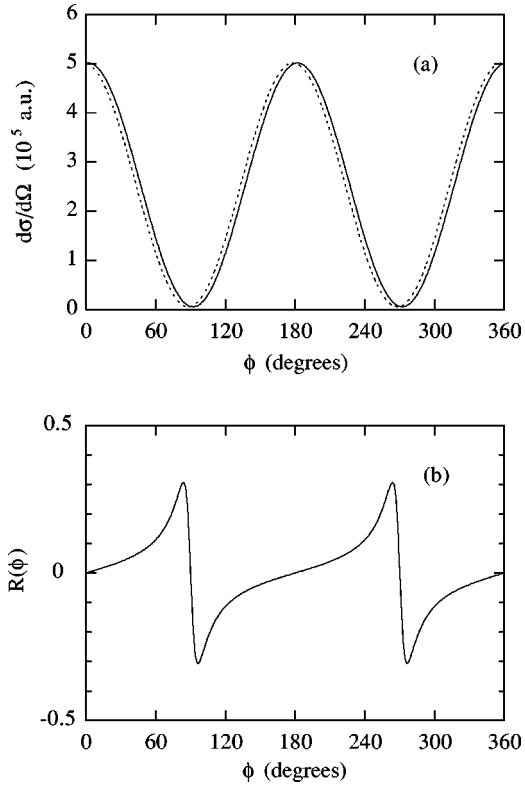


FIG. 5. Same as Fig. 4 with $\omega_H = 11\omega_L$.

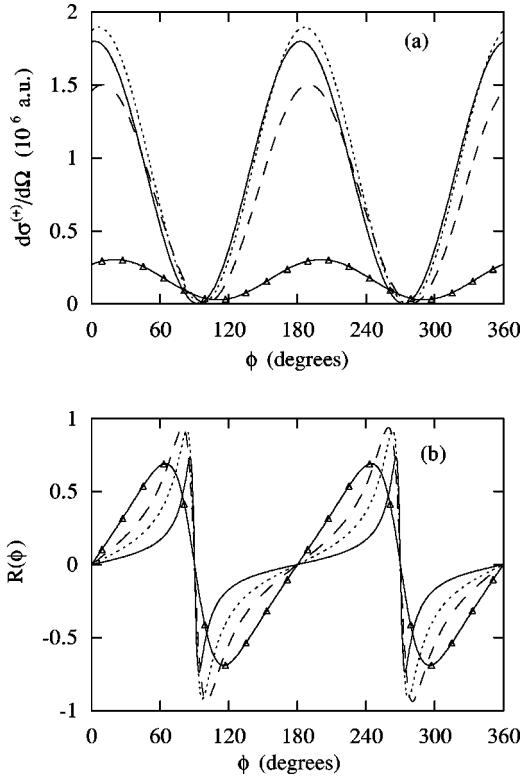


FIG. 6. Same as Fig. 4 for the following three-color process: absorption of harmonic photons with energy $\omega_H = 9\omega_L$, $\omega_H = 11\omega_L$ and absorption/emission, of a laser photon with energy $\omega_L$, the final energy of the photoelectron being $E_0 + 10\omega_L$. (a) The full line corresponds to the differential cross section for right-polarization and a phase difference between the two harmonic fields of 0°; dashed line: 45° of phase difference; dotted line: 90° of phase difference; —△—: 180° of phase difference. (b) Corresponding dichroic signals as defined in Eq. (12).

however less unfavorable than in the preceding case. As an example, for H9, see Figs. 4(a) and 4(b), the dichroic signal is still $R(60°) \approx 0.25$, while the differential cross section is of the order of one-third of its maximum value. Comparing with the Figs. 5(a) and 5(b), one observes that the situation becomes less favorable for higher harmonics, i.e., for faster photoelectrons, as both the cross sections and the dichroic ratio decrease. These results have motivated us to turn to other more adequate scenarios, taking advantage of the unique properties of higher harmonic sources.

### C. Three-color, two-photon ionization

In experiments involving XUV harmonics, another class of phenomena can take place if the atom is irradiated simultaneously by two consecutive harmonics instead of only one [17,18,23]. This can be easily achieved with the harmonic sources as a Dirac comb of frequencies is naturally emitted by atoms when irradiated by the fundamental of the laser. In fact, if the harmonics are not dispersed and selected, it is an easy matter to get several frequencies within the XUV beam. For instance, if the ninth (H9) and the eleventh (H11) harmonics are simultaneously present with the laser, two quantum paths are open to reach a final state with energy $E_0 + 10\omega_L$ via the additional exchange of one laser photon. It is then expected that the dichroic signal should be modified as compared to the case in which only one harmonic is present.

This is shown in Figs. 6(a) and 6(b), where we have reported the $\phi$ dependence of, respectively, the cross section and the dichroic ratio for a laser frequency $\omega_L = 1.55$ eV, in the presence of its harmonics H9 and H11 with equal intensities, and a final photoelectron energy $E_0 + 10\omega_L \approx 1.9$ eV, from hydrogen $(1s)$. As seen in the figures, a new parameter comes into play, namely the relative phase between the harmonics. Depending on this phase difference, the magnitudes and angular distributions are significantly modified [23]. In order to illustrate this point, we have displayed the differential cross sections and ratio $R(\phi)$ for a few selected phase differences. The main result is that the contrast in the dichroic signal can reach values close to unity and, in any case, well over 50%. We note also that, although the maximum contrast is still located at angles close to the minima of the cross sections, there are several angular windows available for securing the observation of sizeable effects. Moreover, comparing Figs. 4(b) and 6(b), where the angular dependences of the dichroic signals for the same final energy state $E_0 + 10\omega_L$ are reported, one can verify that the presence of two harmonics, instead of only one, will significantly enhance the magnitude of the dichroic effect.

Another interesting feature deduced from our simulations is to evidence how much the dichroic signal is sensitive to the phase difference between two consecutive harmonics. This observation might reveal itself as being very useful as it provides an alternative way to determine the relative phases

of high order harmonics, a point which is still under active discussion [24]. We turn now to a brief discussion of higher-order ionization processes in the course of which the atom exchanges more than two photons with the fields.

### III. THREE-PHOTON, TWO-COLOR IONIZATION

If the intensity of the IR laser is high enough, more than one photon $\omega_L$ can be absorbed/emitted simultaneously wth the absorption of the harmonic photon $\omega_H$ [16–18,23]. The simpler scenario is when the atom absorbs two IR photons in addition to the UV harmonic, the photoelectrons being ejected with a kinetic energy: $E_0+2\omega_L+\omega_H$ [25]. The numerical computation has been performed again for the $1s$ hydrogen ground state. Then, as compared to the preceding cases, other angular momentum states are accessible, namely $L=1$ and $L=3$, and new quantum paths are opened, as a consequence of the permutations in the order in which the photons are absorbed. As shown next, these factors can modify significantly the dichroic ratio.

In the simpler case of an initial $s$ state, a general analysis, similar to the one leading to Eq. (6), is easily performed, based on symmetry and rotational invariance, see Ref. [10]:

$$M^{(3)}=\hat{\boldsymbol{\epsilon}}_L\cdot\hat{\mathbf{k}}[a_1\hat{\boldsymbol{\epsilon}}_L\cdot\hat{\boldsymbol{\epsilon}}_H+a_2(\hat{\boldsymbol{\epsilon}}_L\cdot\hat{\mathbf{k}})(\hat{\boldsymbol{\epsilon}}_H\cdot\hat{\mathbf{k}})] + a_3(\hat{\boldsymbol{\epsilon}}_L\cdot\hat{\boldsymbol{\epsilon}}_L)(\hat{\boldsymbol{\epsilon}}_H\cdot\hat{\mathbf{k}}). \quad (15)$$

The atomic parameters $a_j$ are complex quantities expressed in terms of third-order reduced radial amplitudes of the general form:

$$T_{\lambda L}(\omega_I,\omega_J)=\langle R_{k,L}|rG_\lambda(E_0+\omega_I+\omega_J)rG_1(E_0+\omega_I)r|R_{1s}\rangle, \quad (16)$$

where the pairs $\lambda,L=(0,1)$, $(2,1)$, and $(2,3)$, in accordance with dipole selection rules.

For the chosen geometry, see Fig. 1, an expression similar to the one in Eq. (8) can be derived:

$$\frac{d\sigma^{\pm}}{d\Omega(\theta,\phi)}\propto[|a_1|^2+|a_2|^2\sin^4\theta\cos^2\phi + 2\,\mathrm{Re}\{a_1a_2^*\}\sin^2\theta\cos^2\phi \pm \mathrm{Im}\{a_1a_2^*\}\sin^2\theta\sin(2\phi)]\sin^2\theta, \quad (17)$$

More explicitly, the dichroic difference is

$$\frac{d\sigma^+}{d\Omega(\theta,\phi)}-\frac{d\sigma^-}{d\Omega(\theta,\phi)}\propto\mathrm{Im}\{e^{i(\eta_3-\eta_1)}\mathcal{R}_1\mathcal{R}_2^*\}\sin^4\theta\sin(2\phi). \quad (18)$$

The explicit forms of the quantities $\mathcal{R}_J$ are

$$\mathcal{R}_1=T_{23}(\omega_L,\omega_L)+T_{23}(\omega_L,\omega_H)+T_{23}(\omega_H,\omega_L),$$

$$\mathcal{R}_2=6T_{21}(\omega_L,\omega_L)+T_{21}(\omega_L,\omega_H)+T_{21}(\omega_H,\omega_L) + 5[T_{01}(\omega_L,\omega_H)+T_{01}(\omega_H,\omega_L)], \quad (19)$$

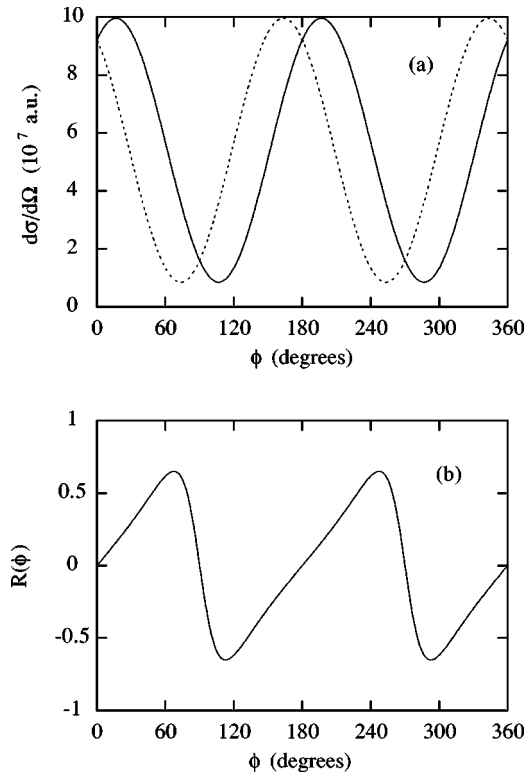


FIG. 7. Differential cross section $d\sigma/d\Omega$ in a.u. and the corresponding dichroic signal $R(\phi)$ as a function of the azimuthal angle $\phi$ for the absorption from the hydrogen atom ground state ($1s$) of two circularly polarized laser photons with energy $\omega_L=1.55$ eV and a linearly polarized harmonic photon with energy $\omega_H=9\omega_L$. The corresponding intensities were taken to be equal to 1 a.u. The geometry is shown in Fig. 1, with $\theta=90°$. (a) The full line corresponds to the differential cross section for right-polarization, while the left-polarization case is shown in dotted line. (b) Dichroic signal as defined in Eq. (10).

This result indicates that for $\theta=\pi/2$, the angular dependence of the the dichroic difference and of the dichroic ratio is similar to that for the two-photon, two-color ionization. However, the magnitude of $R(\phi)$ can be changed as compared with the two-photon case as a result of the different structure of the three-photon radial matrix elements.

A typical example of such a behavior is shown in the Figs. 7(a) and 7(b) where the $\phi$ dependence of the differential cross sections and of the dichroic signal are, respectively, displayed for $\omega_L=1.55$ eV and $\omega_H=9\omega_L$. One observes first that $d\sigma^+$ and $d\sigma^-$ differ more significantly from each other than in the preceding schemes, compare with the Figs. 2–6. Interestingly, it appears that the contrast in the dichroic ratio can reach values larger than 50%. Moreover, as an additional bonus, these maximum values are not located at angles too close to the minima of the angular dependence of the cross section. This clearly opens the possibility of obtaining reliable dichroic signals in angular ranges wider than in the two-photon cases. Note that we have checked that the same overall behavior is observed for this class of processes at other harmonic frequencies.

## IV. CONCLUSIONS

We have explored the potentialities of several scenarios designed to observe circular dichroism effects on unpolarized atomic targets. The schemes considered involve the absorption and exchange of several photons, with distinct polarization states, from different radiation fields. We have chosen to specially address the case in which one of the radiation source is a (linearly polarized) high harmonic of an IR laser, while the other field is the intense (circularly polarized) laser itself. Our motivation is that experiments are currently being planned along these lines [14]. The simulations have been performed for the test-case of the ground-state hydrogen atom, in the perturbative limit, i.e., in the limit of moderate intensities for both the harmonic and the laser.

The main outcome of our simulations is to show that dichroism effects are indeed present in the angular distributions of the photoelectrons. However the simpler process, namely two-color, two-photon ionization, either in standard or in ATI conditions, is not well suited for obtaining useful data as the maxima of the dichroic signal are located close to the minima in the angular distribution of the photoelectrons, i.e., in the regions where the uncertainty in the measurement is likely to be maximum.

In order to alleviate this difficulty we have considered two other scenarios. One of these relies on the characteristic properties of harmonic emission spectra which are constituted of equally spaced lines separated by $2\omega_L$. In the simultaneous presence of two consecutive harmonics and of the laser, three-color two-photon ionization can take place. Then, new interfering quantum paths can lead to a given final state and both the angular distribution of the photoelectrons and the dichroic signal are modified. As compared with the preceding two-color two-photon ionization scheme, our simulations demonstrate that under these new conditions, the observation of dichroism should be much easier in wider angular ranges.

Another scheme exploits the fact that, even at moderate laser intensities, the exchange of several IR photons can take place with relatively high probability. We have considered such a situation in which the atom is ionized through the absorption of one harmonic and of two laser photons. The angular distribution of the photoelectrons and the variations of the dichroic signal are again notably modified as compared to the preceding cases. Moreover, our simulations indicate that the contrast in the dichroic ratio can be larger than in the preceding cases and that the conditions of observability are more favorable.

Natural extensions of the above investigations can be considered in several directions: (i) Changing the geometry (propagation direction of the radiation beams, orientation of the polarization vectors, detection geometry, etc.) can provide complementary information [26]. (ii) If one of the fields is elliptically polarized, new features will be observed in the angular distributions [26]. (iii) At higher laser intensities, a nonperturbative regime will prevail. Then larger numbers of IR photons can be exchanged with the atom and it will be interesting to verify whether or not dichroism effects are blurred when too many quantum paths can lead to a given photoelectron energy state. This question will be addressed in a forthcoming paper.

## ACKNOWLEDGMENTS

Numerous helpful discussions with Dr. P. Agostini are gratefully acknowledged. The Laboratoire de Chimie Physique-Matière et Rayonnement is a Unité Mixte de Recherche, Associée au CNRS, UMR 7614, and is Laboratoire de Recherche Correspondant du CEA, LRC No. DSM-98-16. The support of the INTAS -RFBR Grant No. 97-673 is acknowledged. Parts of the computations have been performed at the Center de Calcul pour la Recherche (CCR, Jussieu, Paris) and at the Institut du Développement et des Ressources en Informatique Scientifique (IDRIS).

[1] See, for instance, G. Schoenhense and J. Hornes, in *VUV and Soft-X-ray Photoionization*, edited by U. Becker and D.A. Shirley (Plenum Press, New York, 1996), p. 607.

[2] J. Berakdar and H. Klar, Phys. Rev. Lett. **69**, 1175 (1992); a recent reference is J. Berakdar, J. Phys. B **32**, L27 (1999).

[3] J. Viefhaus *et al.*, Phys. Rev. Lett. **77**, 3975 (1996); V. Mergel *et al.*, *ibid.* **80**, 5301 (1998); K. Soejima *et al.*, *ibid.* **83**, 1546 (1999).

[4] A. Kheifets and I. Bray Phys. Rev. Lett. **81**, 4588 (1998).

[5] P. Strange, P.J. Durham, and B.L. Gyorffy, Phys. Rev. Lett. **67**, 3590 (1991); C.F. Hague, *et al.*, Phys. Rev. B **48**, 3560 (1993).

[6] M. Bashkansky, P.H. Bucksbaum, and D.W. Schumacher, Phys. Rev. Lett. **60**, 2458 (1988).

[7] P. Lambropoulos and X. Tang, Phys. Rev. Lett. **61**, 2506 (1988); H.G. Muller, G. Petite, and P. Agostini, *ibid.* **61**, 2507 (1988).

[8] N.L. Manakov, in *Super-Intense Atom-Laser Physics IV*, edited by H.G. Muller and M.V. Fedorov (Kluwer Academic Publishers, Dordrecht, 1996), pp. 153.

[9] F. Dulieu, C. Blondel, and C. Delsart, J. Phys. B **28**, 3845 (1995); experimental results are commented on in **28**, 3861 (1995).

[10] N.L. Manakov, A. Maquet, S.I. Marmo, V. Véniard, and G. Ferrante, J. Phys. B **32**, 3747 (1999).

[11] C.N. Yang, Phys. Rev. **74**, 764 (1948).

[12] P. Lambropoulos, Adv. At. Mol. Phys. **12**, 87 (1976).

[13] U. Fano, Phys. Rev. A **32**, 617 (1985).

[14] P. Agostini (private communication).

[15] P. Salières, A. L'Huillier, P. Antoine, M. Lewenstein, Adv. At., Mol., Opt. Phys. **41**, 89 (1999).

[16] V. Véniard, R. Taïeb, and A. Maquet, Phys. Rev. Lett. **74**, 4161 (1995).

[17] J.M. Schins *et al.*, J. Opt. Soc. Am. B **13**, 197 (1996); A. Bouhal *et al.*, *ibid.* **14**, 950 (1997); A. Bouhal *et al.*, Phys. Rev. A **58**, 389 (1998).

[18] T.E. Glover *et al.*, Phys. Rev. Lett. **76**, 2468 (1996).

[19] A review article on the Coulomb Green's functions is: A.

Maquet, V. Véniard, and T.A. Marian, J. Phys. B **31**, 3743 (1998).
[20] N.L. Manakov and A.V. Meremianin, Zh. Exp. Teor. Fiz., **111**, 1984 (1997) [Sov. Phys. JETP **84**, 1080 (1997)].
[21] R. Taïeb, V. Véniard, A. Maquet, S. Vucic, and R. Potvliege, J. Phys. B **24**, 3229 (1991).
[22] E.P. Wigner, Phys. Rev. **73**, 1002 (1948); for a discussion in the context of multiphoton ionization, see A. Maquet, Phys. Rev. A **15**, 1088 (1977).
[23] V. Véniard, R. Taïeb, and A. Maquet, Phys. Rev. A **54**, 721 (1996).
[24] P. Balcou, A.S. Dederichs, M.B. Gaarde, and A. L'Huillier, J. Phys. B **32**, 2973 (1999).
[25] M. Fifirig, A. Cionga, and V. Florescu, J. Phys. B **30**, 2599 (1997).
[26] N.L. Manakov *et al*. (private communication).